02

Effect of Internal Charging on Cathodoluminescence Profiling Capability: Boron-Implanted β-Ga_2O_3

© A.A. Tatarintsev[1,2], A.E. Ieshkin[1], E.Yu. Zykova[1], N.G. Orlikovskaya[1], V.A. Kiselevskiy[2,3]

[1] Moscow State University, Moscow, Russia
[2] National Research Center „Kurchatov Institute“, Moscow, Russia
[3] Institute of Ultrahigh Frequency Semiconductor Electronics of the Russian Academy of Sciences, Moscow, Russian
e-mail: tatarintsev@physics.msu.ru

Received December 05, 2024
Revised December 09, 2024
Accepted December 10, 2024

The effect of sample electrification by an electron beam on the integral intensity of cathodoluminescence and on the shape of the emission spectrum is investigated in the work. For this purpose, using the example of Fe : β-Ga_2O_3 implanted with boron, the results of cathodoluminescence measurements are compared for three series of experiments: when the surface of the sample under study was not grounded, grounded, or covered with a conductive grounded film. The studies have shown that even when using a metal film, the accumulation of charge under it can distort the shape of the spectrum. Such a distortion of the spectra during a cathodoluminescence study with depth resolution will lead to an incorrect determination of the defect concentration profiles. Comparison of the spectra sequentially recorded with an increase in the electron beam energy and then with a decrease in energy can be proposed as a quick criterion for assessing the effect of charging on the quality of luminescent center profiling.

Keywords: gallium oxide, cathodoluminescence, internal charging, boron implantation, defect profiling.

DOI: 10.61011/EOS.2025.03.61155.139-24

Introduction

Gallium oxide is a promising material for medium- and high-power electronics [1], so in recent years there has been an increasing number of publications devoted to the study of this wide-gap semiconductor[1–7]. The interest in this material is primarily driven by its unique properties, which make it promising for a range of advanced applications. The wide band gap (4.8 eV for β-Ga_2O_3) is an important advantage of gallium oxide, which significantly reduces the generation of free current carriers and hence leads to an increase of the critical breakdown field E_C to 8.7 MV/cm [1].

Ion implantation and subsequent activation annealing are important technological processes for the creation of semiconductor devices. These processes make it possible to form the required distribution of the introduced impurity, which is necessary to obtain devices with specified properties. Thermal annealing is used to activate the atoms of the alloying impurity and eliminate defects arising from the implantation process. At the same time, it can cause diffusion of implanted atoms as well as the evolution of point defects [8–10], so it is necessary to study the distribution of impurities in the sample after implantation and annealing.

At present, implantation of boron ions into various semiconductors (Si, GaN) is widely used to create various semiconductor devices [11]. The doping of gallium oxide with boron is of broad scientific and practical interest. For example, high concentrations of boron are expected to be used to make slow neutron detectors [12]. Despite this, boron is one of the least studied impurities in Ga_2O_3. Boron ions are isovalent impurities and replace gallium in the crystal lattice. The distribution of boron atoms in gallium oxide after implantation and annealing was studied in Ref. [12]. It was shown that after high-temperature annealing, the depth distribution profile of boron concentration has two maxima. It should be noted that such a distribution is characteristic of samples subjected to postimplantation annealing and was found, for example, when implanting small aluminum clusters into silicon [13]. In the case of gallium oxide in the region of the first maximum at a depth of ~ 50 nm below the surface, boron atoms are not located in the nodes of the gallium sublattice, but are part of boron-containing complexes such as B_xO_y, $B-Ga_{v-O}$ or form precipitates of elementary boron. Iron doping is used to create a semi-insulating material [14]. Iron creates a deep acceptor level that is 0.8 eV below the bottom of the conduction band. The triple acceptor level is also a gallium vacancy, whose energy levels are located 3 and 3.3 eV above the valence band ceiling [15]. The development of devices based on Ga_2O_3 requires not only the knowledge of the depth distribution of impurities introduced by implantation, but it also necessary to understand the mechanisms of defect formation and their nature. Multiple defects may be present in source gallium oxide, the number and type of which vary with growth and processing [10,16–18].

However, the nature of intrinsic point defects in Ga_2O_3 has not been practically studied [15]. Cathodoluminescence spectroscopy is a well-established method for detecting optically active defects. In a cathodoluminescence study, the sample is irradiated with electrons with energy of $1-30$ keV, which can lead to excitation of valence band

electrons to higher levels or to the conduction band with subsequent relaxation by radiative or non-radiative pathways. Cathodoluminescence (CL) spectra are caused by the radiative transitions of electrons involving levels inside the band gap or as a result of interband transitions and carry information about optically active levels of the material under study. Levels within the band gap can arise from intrinsic and impurity defects [1,3].

A cathodoluminescence study with depth resolution [19] can provide useful information on the distribution of impurities and defects in a solid. For this purpose, CL spectra are recorded with a gradual increase in the excitation electron energy. An increase of energy leads to an increase of the penetration depth of the primary electrons and, consequently, to an increase of the depth of the CL yield region [20]. At the same time, electron irradiation of nonconducting samples can lead to the formation of a negative potential near the surface, which will change the effective energy of the probing electron beam.

The influence of electrification of the sample by the electron beam on both the integral CL intensity and the shape of its spectrum was studied in this paper. Usually, when studying dielectric samples to neutralize the charging effect, the samples are covered with conductive films (carbon or metal), but even in this case, electrons passing through the film can accumulate in the dielectric volume. The electric fields created by the accumulated charge can distort the profiling results. Therefore, the results of three experimental series were compared in this paper — the sample surface is ungrounded, grounded, and covered with a conductive grounded film during the measurement of CL spectra. The studies were carried out on an example of iron-doped wide-gap semiconductor β-Ga_2O_3 implanted with boron.

Samples and experimental methods

Semi-insulating plates of β-Ga_2O_3 with substrate orientation (-201) doped with iron during crystal growth. The bandgap width of β-Ga_2O_3 is $E_g = 4.8-4.9$ eV [1,21], with the indirect transition 0.1 eV smaller.

Two samples of β-Ga_2O_3 implanted with boron at different doses (implantation was conducted in Lobachevsky State University of Nizhny Novgorod) were studied [12]. Sample B1 was implanted with boron with 40 keV energy and fluence of 10^{15} cm^{-2}, and sample B2 was sequentially implanted with boron ions with 14 keV energy with fluence of $3.6 \cdot 10^{15}$ cm^{-2}, 22 keV with fluence of $1.8 \cdot 10^{15}$ cm^{-2} and 40 keV with fluence of $1.9 \cdot 10^{16}$ cm^{-2}. Both samples were annealed at 950°C in nitrogen atmosphere for 30 min. For sample B2, the thickness of the boron implanted layer was ~ 170 nm, the concentration of boron atoms was $2 \cdot 10^{21}$ cm^{-3}, which corresponds to $\sim 5\%$ of the concentration of Ga atoms in Ga_2O_3. The implanted layer thicknesses and boron atom concentration data were calculated using SRIM program and experimentally measured by secondary ion mass spectrometry (SIMS) [12]. The resistance of the surface layer was ~ 14 kΩ/cm^2 after implantation and subsequent annealing.

The CL spectra were recorded in a Varian ultrahigh-vacuum chamber, the pressure in which during measurements was 10^{-8} Torr. Gallium oxide samples were irradiated with a defocused electron beam with a diameter of ~ 1.7 mm and a current 30 μA (the current density was $1.3 \cdot 10^{-3}$ A/cm^2, which corresponds to the electron flux density $\varphi = 8.3 \cdot 10^{15}$ el/cm^{2}s). The maximum accelerating voltage of the electron gun was limited to 3 kV in our experiments. An additional positive potential was applied to the entire table on which the samples were secured to accelerate the electrons to the required energy. CL spectra were taken in the range of electron energies 1–20 keV, first when the electron energy was increased from the minimum to the maximum value (forward pass) and then when the energy was decreased (backward pass). The spectra were recorded using an Ocean STS–VIS microspectrometer with a CCD array in the wavelength range of 350–850 nm, following the experimental procedures described in Ref. [22,23]. The spectrum accumulation time was 10 s.

Three methods were used in our experiments to mount the samples. In first series of experiments, samples were mounted with conductive tape with the non-implanted side facing the metal holder. This method prevented any runoff of charges from the surface. Thus, this method produced an ungrounded „film“ (i.e., boron implanted layer) on a semi-insulating layer of Fe:β–Ga_2O_3. We will refer to this method of mounting the sample as ungrounded. In the second series of experiments, the samples were similarly mounted on the holder using double-sided conductive tape (non-implanted side facing out), with the addition of conductive tape to enable surface charge runoff. Hereinafter, we will use the term „grounded“ for experiments with such samples. After the second experiment, a thin conductive Au film was applied to the samples to reduce the surface resistance and charge runoff from the surface, as is usually done in the study of dielectric samples. The thickness of the film was selected so that the surface of the sample was transparent for CL registration, but the film was continuous. The film was applied using a JEOL JFC-1100 cathode sputtering system. The film thickness was measured on a chipped surface of the witness plate using a scanning electron microscope and was ~ 14 nm. In the third experiment, the samples were mounted similarly to the grounded samples — additionally, a conductive tape was used to ensure charge runoff from the film onto the metal table.

After depositing a metallic film on the sample surface, the overall cathodoluminescence intensity significantly decreases due to optical absorption. The transmission coefficients of gold films with different thicknesses are provided in Ref. [24]. Some of the energy of the primary electrons is lost as electrons pass through the thin film. The average energy of the passed electrons can be estimated

according to Ref. [25] using the expression

$$\bar{E}_{\text{eff}} = cE_0 \exp\left(-\frac{x}{R}\right),$$

where x is the film thickness, $R = 90\rho^{-0.8}E_0^{1.3}$ (for $E_0 < 10\,\text{keV}$) or $R = 45\rho^{-0.9}E_0^{1.7}$(for $E_0 \geq 10\,\text{keV}$) is the maximum depth of electron travel in the material. The proportionality constant can be estimated as

$$c = \frac{1 + 0.5\eta_B + 0.5\eta_B^2}{1 + \eta_B},$$

where η_B is the coefficient of reflection of electrons from the material. For experiments performed on film samples, all results are presented as a function of the average energy of the passed electrons.

The recorded spectra represented the dependence of the radiation intensity on the wavelength $I_{\text{CL}}(\lambda)$, so the intensity was recalculated using the formula $I_{\text{CL}}(E) = I_{\text{CL}}(\lambda)\lambda^2/hc$ when processing the experimental results [26]. The decomposition of the spectra into Gaussian components was performed after recalculation.

Experimental data and discussion

Change of the signal intensity

The intensity of the CL signal is determined by the number of electron-hole pairs generated by the electron beam, the concentration of luminescent centers, the probability of electron capture on the luminescent centers, and the center lifetime [27]. Thus, three fundamental processes are involved in the formation of cathodoluminescent radiation: generation of charge carriers, their motion, and recombination [20]. In the case of a uniform distribution of the concentration of luminescent centers, if the average number of incoming electrons during the lifetime of traps is much larger than the number of these centers, the intensity of the CL signal should increase with increasing energy. Indeed, cathodoluminescent radiation will be generated in an increasingly larger volume containing an increasing number of luminescent centers. However, when the defects are not uniformly distributed, the situation is more complicated. It can be described by dividing it into layers of equal concentrations and taking into account the concentration of electron-hole pairs in these layers [19]. Let us consider how the total CL intensity of boron-implanted gallium oxide varies for different primary electron beam energies.

At low electron beam energies, the CL intensity for the ungrounded sample changes weakly (curve *1* in Fig. 1), but at electron beam energies above 10 keV for B1 and 14 keV for B2, the intensity sharply increases. It should be noted that the intensity change occurs almost instantaneously upon reaching this energy and is accompanied by instability in the intensity and discharges on the surface observed visually.

The sharp increase in the CL intensity of the ungrounded sample observed during direct passage is probably due to electrostatic breakdown of the semi-insulating substrate on the sample holder. In resulting breakdown, the accumulated charge can flow down the resulting breakdown channel, resulting in a decrease in surface potential and a decrease in internal electrostatic fields. In this case, the actual energy of the incident electrons increases to the nominal energy, and thus the depth of their penetration into the sample increases. If, after reaching the maximum electron beam energy (18 keV), the energy is decreased, the CL intensity of sample B2 returns to its previous value only at an electron energy of 8 keV. That is, there is a kind of energy hysteresis, which is clearly visible in the curve *1* in Fig. 1, *b*. The decrease of the CL intensity at 8 keV is not sharp, but relatively smooth. This gradual decrease in intensity is due to the gradual increase in surface potential during electron irradiation after the electron energy is insufficient to sustain breakdown. In this case, the shape of the spectrum practically does not change with the irradiation time. This may indicate the same defect distribution profile in the near-surface region. The drop of the intensity of all CL lines is associated here with a decrease in the depth of primary electrons (and, consequently, in the output region of the cathodoluminescent signal) due to a decrease of their actual energy as a result of an increase in the charge potential of the surface with irradiation time. If the emission centers were not uniformly distributed in depth, one would expect the spectra to be distorted during the charging process.

The CL intensity of the grounded sample increases relatively smoothly with the increase of the excitation electron energy (curve *2* in Fig. 1). However, the intensity is significantly lower for the energy backward pass (dashed lines in Fig. 1) than for the forward pass. This may be attributable to the charge effect caused by the internal charging of gallium oxide when the underlying layer of semi-insulating gallium oxide captures electrons to the deep acceptor levels of iron. Electrons with energy 14–18 keV penetrate to a depth of 1–1.5 μm, where the negative charge accumulates. This intrinsic charge distribution will generate fields that can reduce the electron interaction region, reduce the electron drift region, and generally spread out the opposite charges of electron-hole pairs, resulting in a reduced CL intensity for the sample.

When a grounded conductive film is applied to the sample surface, the electric fields do not affect the approaching electron beam. But, as can be seen from the experimental data, even in this case the difference of CL intensity at forward and backward passes still exists. The decrease of CL intensity during backward passage is also caused by the internal charge distribution under the conductive film [28].

Shape distortion of CL spectra

Different CL lines may have different excitation mechanisms and may also be associated with luminescent centers having different depth distributions. Therefore, as a result of charge accumulation in the sample volume, not only the intensity of the spectrum may change, but also its

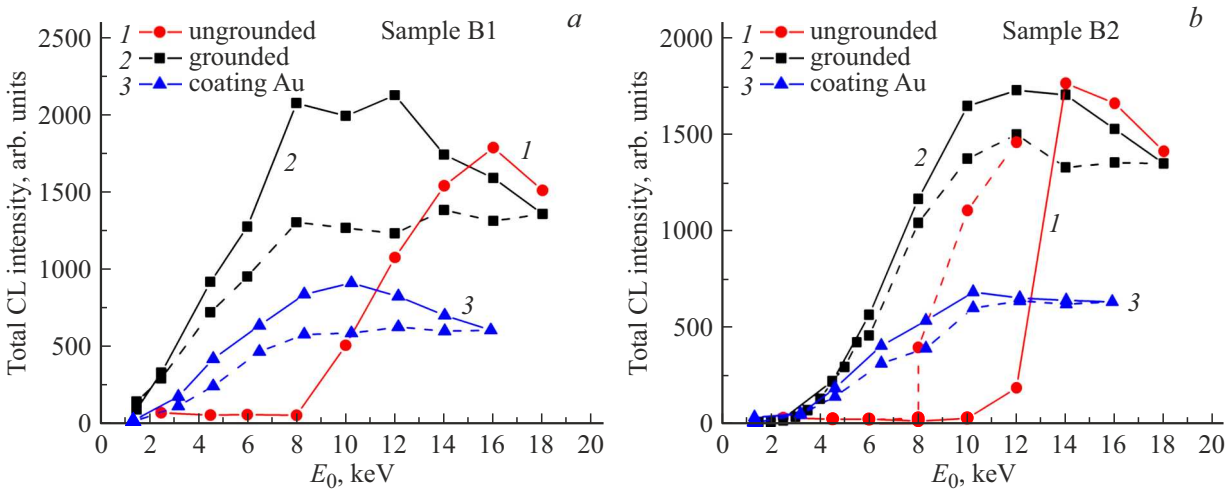

Figure 1. The dependence of the total CL intensity on the electron beam energy for samples B1 (*a*) and B2 (*b*) for the cases when the sample surface was ungrounded (1), grounded (2), coated with Au film and grounded (3). The dashed lines indicate the energy reversal — when the energy decreased from the maximum value to the minimum value.

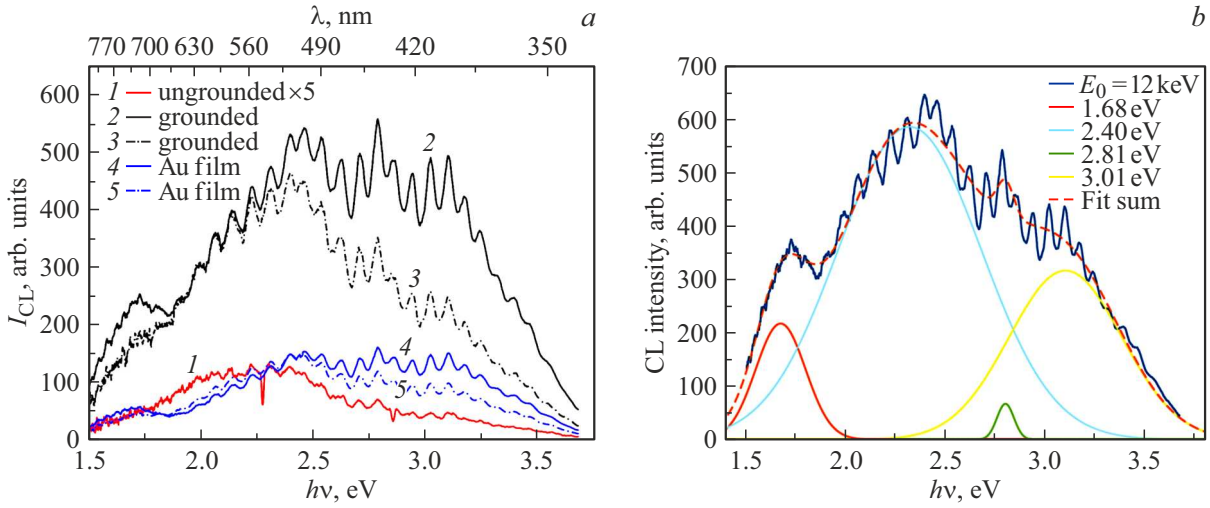

Figure 2. (*a*) -CL spectra of sample B1 recorded at electron energy of 8 keV: *1* — for the ungrounded sample (spectrum increased by 5 times), *2, 3* — for the grounded sample, *4, 5* — for the sample coated with a gold film; solid curves — forward pass in energy, dashed curves — backward pass. (*b*) Gaussian curve expansion of the CL spectrum of a grounded sample B_1, electron energy 12 keV, direct pass.

shape may change. Fig. 2, *a* shows the CL spectra of sample B1 for all three experiments at excitation electron energies $E_0 = 8$ keV. It can be seen that, for the grounded sample, the shape of the spectrum changes strongly when the CL spectra are taken with the forward (spectrum *2*) and backward (spectrum *3*) passes. The same behavior of the spectra is observed for the sample coated with a conducting film (spectra *4* and *5*). Here, the energy of the electron beam incident on the sample was 10 keV, but considering the above calculations, the effective average energy of the electrons that passed through the film was $E_{ef} = 8.3$ keV. For the ungrounded sample (spectrum *1*), the CL intensity was very low, increasing only at incident electron energies exceeding 10 keV.

It should be noted that after reaching the value of the primary beam energy at which the CL intensity for the ungrounded sample sharply increases, the shapes of the spectra become similar to each other.

The measured CL spectra for all samples and all excitation electron energies were decomposed into Gaussian curves and the integral intensities of the spectral lines were determined. 4–5 lines are commonly used for the decomposition of gallium oxide CL spectra [6,15,29–32] . Taking into account the papers [1,6,29,33] we have chosen the following four lines, which best describe all the experimental spectra obtained.

1. Ultraviolet line with energy of 3.1 eV (400 nm) associated with donor-acceptor transitions [34,35].

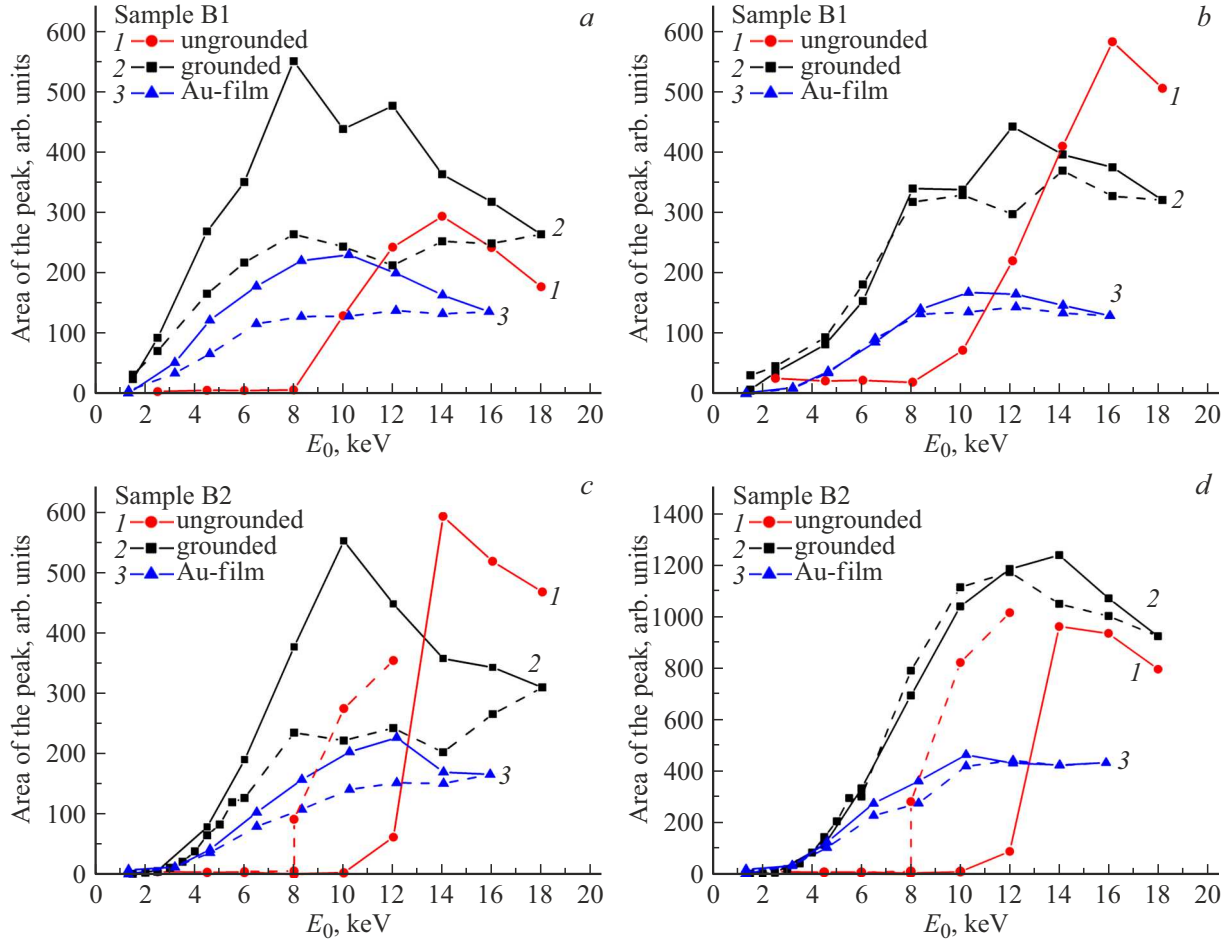

Figure 3. The intensity dependence of the Gaussian peaks at energies 3.1 (*a*, *c*) and 2.4 eV (*b*, *d*) for samples B1 (*a*, *b*) and B2 (*c*, *d*) at „direct“ (solid line) and „reverse“ (dashed line) energy passes: *1* — the surface is not grounded, *2* — the surface is grounded, *3* — the surface is covered with Au film and grounded.

2. The blue line ~ 2.8 eV (430 nm), also attributed to donor-acceptor pair transitions [34,35].

3. Green line 2.4 eV (496 nm) associated with an isolated gallium vacancy V_{Ga} [32].

4. The red line with energy ~ 1.7 eV (700 nm).

Fig. 2, *b* shows the decomposition of the CL spectrum of the grounded sample B1 taken with the excitation electron energy of $E_0 = 12$ keV. The spectrum is recorded at direct passage.

After decomposition into Gaussian components of all CL spectra of samples B1 and B2, the dependences of the area of Gaussian peaks (i.e., their intensity) on the primary electron beam energy were plotted. Fig. 3 shows examples of such dependencies for lines 3.1 and 2.4 eV. The dependences of intensity on the average energy of electrons passing through the film are presented for the sample under the gold film. It can be seen that the character of change in luminescence intensity is different. Thus, the intensities of the 3.1 eV line at the forward and backward passes differ markedly, and this difference is noticeable even in the case of the sample coated with a metal film. This should be considered when using depth-resolved CL spectroscopy to reconstruct the defect distribution profile. Since under the action of electric fields created by the accumulated charges, the intensity of different lines behaves differently, the final result of defect profile reconstruction will be incorrect.

At the same time, the intensity of the 2.4 eV line for samples with grounded surface and with metal film is practically reproducible for both forward and backward passes. For the ungrounded sample, hysteresis remains in the case of this line, and its intensity appears to be higher on the backward pass than on the forward pass.

As noted in the previous paragraph, the depth distributions of the defects emitting different lines are assumed to be the same. Why do the depth dependences of the intensity of these lines appear to be different?

The different behavior of the lines in the CL spectrum at forward and backward passages can be explained by the different nature of these lines. Indeed, the lines 2.8, 3.1 eV are associated with the donor-acceptor transition, which requires first the capture of electrons and holes to the corresponding donor and acceptor levels, and then their

radiative recombination. The 2.4 eV line is associated with an isolated gallium vacancy, which emits a photon when a hole is trapped. The accumulation of negative charge under the implanted film will create internal fields that will affect the drift regions of electrons and holes and separate them in space, which may lead to a reduced probability of their recombination. This will reduce the intensity of the lines in the spectrum associated specifically with the donor-acceptor transition.

An electric field is generated above the ungrounded sample, which inhibits the electrons, reducing their energy and hence their area of interaction with the sample. In the case of a grounded specimen or a specimen under a metallic grounded film, this reduction in the energy of the primary electrons occurs already inside the specimen, and due to the leakage of charge through the grounded surface, this field is much weaker. This suggests that the main reason for the distortion of the spectra of the cathodoluminescent signal is the change in the regions of charge carriers diffusion.

Conclusion

One of the traditional ways to avoid electrification of non-conductive samples, which occurs when they are examined by electron microscope, CL or X-ray microanalysis, is to apply a thin conductive film to the surface. The gallium oxide CL studies performed in the present work have shown that even when a metal film is used, the accumulation of charge under it can distort the shape of the spectrum. The internal electric fields created by the accumulated charge change the area of charge carriers diffusion and, consequently, the volume in which their recombination occurs, as well as lead to the separation of electrons and holes and reduce the probability of their recombination. Distortion of the spectra in a depth-resolved cathodoluminescence study will lead to incorrect determination of defect concentration profiles.

Comparison of spectra sequentially taken at increasing electron beam energy and then at decreasing energy can be proposed as a quick criterion for evaluating the effect of charging dielectric and semiconductor samples on the quality of luminescent center profiling. We emphasize that the conclusions drawn are relevant not only for gallium oxide, but also for any weakly conducting samples in cathodoluminescence studies or X-ray microanalysis.

Acknowledgments

We would like to thank A.A. Nikolskaya, D.I. Tetelbaum, and D.S. Korolev (Lobachevsky State University of Nizhny Novgorod) for providing the samples.

The study was supported by a grant from the Russian Science Foundation №23-22-00083 (https://rscf.ru/project/23-22-00083.

Conflict of interest

The authors declare that they have no conflict of interest.

References

[1] M.D. McCluskey. J. Appl. Phys., **127**, 101101 (2020). DOI: 10.1063/1.5142195

[2] A.I. Titov, K. V. Karabeshkin, A.I. Struchkov, V.I. Nikolaev, A. Azarov, D.S. Gogova, P.A. Karaseov. Vacuum, **200**, 111005 (2022). DOI: 10.1016/j.vacuum.2022.111005

[3] A Nikolskaya, E. Okulich, D. Korolev, A. Stepanov, D. Nikolichev, A. Mikhaylov, D. Tetelbaum, A. Almaev, C.A. Bolzan, A. Buaczik, R. Giulian, P.L. Grande, A. Kumar, M. Kumar, D. Gogova. J. Vac. Sci. Technol. A, **39**, 030802 (2021). DOI: 10.1116/6.0000928

[4] M. Oda, R. Tokuda, H. Kambara, T. Tanikawa, T. Sasaki, T. Hitora. Appl. Phys. Express, **9**, 021101 (2016). DOI: 10.7567/APEX.9.021101

[5] S.J. Pearton, F. Ren, M. Tadjer, J. Kim. J. Appl. Phys., **124**, 220901 (2018). DOI: 10.1063/1.5062841

[6] V. Nikolaev, A.Y. Polyakov, V. Krymov, S. Shapenkov, P. Butenko, E. Yakimov, A. Vasilev, I. Shchemerov, A. Chernykh, N. Matros, L. Alexanyan, A. Kochkova, S.J. Pearton. ECS J. Solid State Sci. Technol., **13**, 015003 (2024). DOI: 10.1149/2162-8777/ad1bda

[7] A.Y. Polyakov, N.B. Smirnov, I. V. Shchemerov, S.J. Pearton, F. Ren, A. V. Chernykh, P.B. Lagov, T. V. Kulevoy. APL Mater., **6**, 096102 (2018). DOI: 10.1063/1.5042646

[8] R. Sharma, M.E. Law, C. Fares, M. Tadjer, F. Ren, A. Kuramata, S.J. Pearton. AIP Adv., **9**, 085111 (2019). DOI: 10.1063/1.5115149

[9] R. Sharma, M.E. Law, M. Xian, M. Tadjer, E.A. Anber, D. Foley, A.C. Lang, J.L. Hart, J. Nathaniel, M.L. Taheri, F. Ren, S.J. Pearton, A. Kuramata. J. Vac. Sci. Technol. B, **37**, 051204 (2019). DOI: 10.1116/1.5118001

[10] R. Sugie, T. Uchida, A. Hashimoto, S. Akahori, K. Matsumura, Y. Tanii. Appl. Phys. Express, **13**(12), 126502 (2020). DOI: 10.35848/1882-0786/abca7c

[11] L. Williams, E. Kioupakis. Appl. Phys. Lett., **111**, 211107 (2017). DOI: 10.1063/1.4997601

[12] A.A. Nikolskaya, D.S. Korolev, V.N. Trushin, M.N. Drozdov, P.A. Yunin, E.A. Pitirimova, A. V. Kudrin, E. V. Okulich, V.I. Okulich, A.N. Mikhaylov, D.I. Tetelbaum. Nucl. Instr. Meth. Phys. Res. B, **537**, 65 (2023). DOI: 10.1016/j.nimb.2023.01.014

[13] X. Zeng, V. Pelenovich, A. Ieshkin, A. Danilov, A. Tolstogouzov, W. Zuo, J. Ranjana, D. Hu, N. Devi, D. Fu, X. Xiao. Rapid Commun. Mass Spectrom., **33** (18), 1449 (2019). DOI: 10.1002/rcm.8489

[14] A.Y. Polyakov, N.B. Smirnov, I. V. Shchemerov, S.J. Pearton, F. Ren, A. V. Chernykh, A.I. Kochkova. Appl. Phys. Lett., **113**, 142102 (2018). DOI: 10.1063/1.5051986

[15] H. Gao, S. Muralidharan, N. Pronin, M.R. Karim, S.M. White, T. Asel, G. Foster, S. Krishnamoorthy, S. Rajan, L.R. Cao, M. Higashiwaki, H. Von Wenckstern, M. Grundmann, H. Zhao, D.C. Look, L.J. Brillson. Appl. Phys. Lett., **112** (24), 242102 (2018). DOI: 10.1063/1.5026770

[16] J. Lee, E. Flitsiyan, L. Chernyak, S. Ahn, F. Ren, L. Yuna, S.J. Pearton, J. Kim, B. Meyler, J. Salzman. ECS J. Solid State Sci. Technol., **6**(2), Q3049 (2017). DOI: 10.1149/2.0101702jss

[17] S. Rafique, L. Han, H. Zhao. Phys. St. Sol. Appl. Mater. Sci., **214**(8), 1700063 (2017). DOI: 10.1002/pssa.201700063

[18] P. Ravadgar, R.-H. Horng, S.-D. Yao, H.-Y. Lee, B.-R. Wu, S.-L. Ou, L.-W. Tu. Opt. Express, **21**(21), 24599 (2013). DOI: 10.1364/oe.21.024599
[19] R. Renoud, F. Papin, J. P. Ganachaud, J. Bigarré. Phys. St. Sol. Appl. Mater. Sci., **203**(3), 591 (2006). DOI: 10.1002/pssa.200521482
[20] V.I. Petrov. UFN, **166**(8), 859 (1996) (in Russian). DOI: 10.3367/UFNr.0166.199608c.0859 [V.I. Petrov. Phys. Usp., **39**, 807 (1996). DOI: 10.1070/PU1996v039n08ABEH000162].
[21] F. Alema, B. Hertog, O. Ledyaev, D. Volovik, G. Thoma, R. Miller, A. Osinsky, P. Mukhopadhyay, S. Bakhshi, H. Ali, W. V. Schoenfeld. Phys. St. Sol., **214**(5), 1600688 (2017). DOI: 10.1002/pssa.201600688
[22] A.A. Tatarintsev, E.Yu. Zykova, A.E. Ieshkin, N.G. Orlikovskaya, E.I. Rau. FTT, **65**(8), 1288 (2023) (in Russian). DOI: 10.61011/EOS.2025.03.61155.139-24 [A.A. Tatarintsev, E.Y. Zykova, A.E. Ieshkin, N.G. Orlikovskaya, E.I. Rau. Physics of the Solid State, **65**(8), 1236 (2023). DOI: 10.61011/EOS.2025.03.61155.139-24].
[23] E.Y. Zykova, A.E. Ieshkin, N.G. Orlikovskaya, A.A. Tatarintsev, V.V. Khvostov, Y.V. Balakshin. Radiat. Phys. Chem., **217**, 111481 (2024). DOI: 10.1016/j.radphyschem.2023.111481
[24] A. Axelevitch, B. Gorenstein, G. Golan. Phys. Procedia, **32**, 1 (2012). DOI: 10.1016/j.phpro.2012.03.510
[25] H.J. Fitting. J. Electron Spectros. Relat. Phenomena, **136**(3), 265 (2004). DOI: 10.1016/j.elspec.2004.04.003
[26] Y. Wang, P.D. Townsend. J. Lumin., **142**, 202 (2013). DOI: 10.1016/j.jlumin.2013.03.052
[27] M.R. Phillips. Microchim. Acta, **155**, 51 (2006). DOI: 10.1007/s00604-006-0506-0
[28] H.G. Orlikovskaya, E.Y. Zykova, A.A. Tatarintsev. Poverkhnost. Rentgenovskie, sinkhrotronnye i neitronnye issledovaniya, **9**, 50 (2024) (in Russian).
[29] Y. Wang, P.T. Dickens, J.B. Varley, X. Ni, E. Lotubai, S. Sprawls, F. Liu, V. Lordi, S. Krishnamoorthy, S. Blair, K.G. Lynn, M. Scarpulla, B. Sensale-Rodriguez. Sci. Rep., **8**, 18075 (2018). DOI: 10.1038/s41598-018-36676-7
[30] A.Y. Polyakov, N.B. Smirnov, I. V. Shchemerov, E.B. Yakimov, V.I. Nikolaev, S.I. Stepanov, A.I. Pechnikov, A. V. Chernykh, K.D. Shcherbachev, A.S. Shikoh, A. Kochkova, A.A. Vasilev, S.J. Pearton. APL Mater., **7**, 051103 (2019). DOI: 10.1063/1.5094787
[31] A.Y. Polyakov, I.H. Lee, N.B. Smirnov, E.B. Yakimov, I.V. Shchemerov, A. V. Chernykh, A.I. Kochkova, A.A. Vasilev, P.H. Carey, F. Ren, D.J. Smith, S.J. Pearton. APL Mater., **7**, 061102 (2019). DOI: 10.1063/1.5109025
[32] Y. Nie, S. Jiao, S. Li, H. Lu, S. Liu, S. Yang, D. Wang, S. Gao, J. Wang, Y. Li. J. Alloys Compd., **900**, 163431 (2022). DOI: 10.1016/j.jallcom.2021.163431
[33] H.H. Tippins. Phys. Rev., **137**, 3A (1965). DOI: 10.1103/PhysRev.137.A865
[34] L. Binet, D. Gourier. J. Phys. Chem. Solids, **59**(8), 1241 (1998). DOI: 10.1016/S0022-3697(98)00047-X
[35] T.T. Huynh, L.L. C. Lem, A. Kuramata, M.R. Phillips, C. Ton-That. Phys. Rev. Mater., **2**(10), 105203 (2018). DOI: 10.1103/PhysRevMaterials.2.105203

Translated by A.Akhtyamov